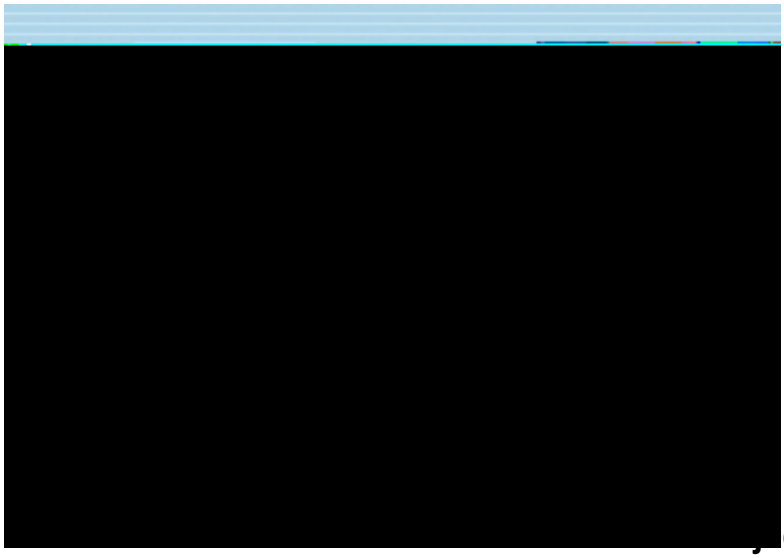

ct

Deliverable D7.2

Demonstration Results

Project acronym: AIRobots
Innovative Aerial Service Robots for Remote Inspections by Contact
Grant agreement no: FP7 248669
Project web site: www.airobots.eu

Due date: 31/1/2013	**Submission date: 05/2/2013**
Start date of project: February 1, 2010	**Duration: 36 months**
Lead beneficiary: AIR-ETHZ	**Revision: 1**

Nature: R	**Dissemination level: PU**
R = Report	PU = Public
P = Prototype	PP = Restricted to other programme participants (including the Commission Services)
D = Demonstrator	RE = Restricted to a group specified by the consortium (including the Commission Services)
O = Other	CO = Confidential, only for members of the consortium (including the Commission Services)

Executive Summary

This deliverable constitutes a preliminary summary of the demonstration activities to be carried out during the final review of the AIRobots project. The targeted experiments are summarized in relation to the individual inspection tasks to be simulated with each flight test and initial results are presented.

TABLE OF CONTENTS

1 **Introduction** 3

2 **Vision-Based Inspection** 3

3 **Tele-Operated Inspection** 6

4 **Surface Scanning by Contact** 8

5 **Aerial Manipulation** 11

6 **Conclusion** 13

1 Introduction

In preparation of the final AIRobots demonstrations a set of four inspection related experiments are summarized in the following. The corresponding flight tests are separated into visual inspection, tele-operated inspection, surface scanning by contact and aerial manipulation.

2 Vision-Based Inspection

Localization and Visual Inspection

This experiment will demonstrate our motion estimation capabilities. Although the experiment will be conducted in the mock-up environment, it will not rely on an external tracking system. As in a real, industrial deployment of the vehicle, motion estimation will rely only on sensors carried on-board (in this case cameras and inertial measurement units). The quad-rotor shown in Fig. 1 will be used for this experiment.

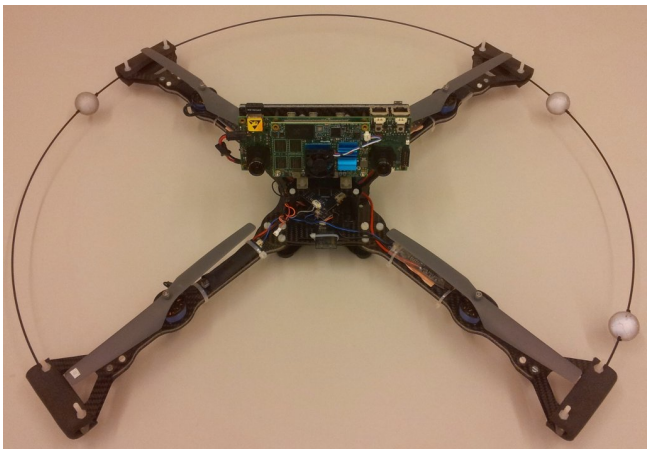

Figure 1: Quad-rotor test vehicle that will be used during the demonstration.

The following two tests will performed:

- *Hovering*: The vehicle will hold a constant reference pose as accurately as possible. This is a key performance indicator and relevant for a real deployment of the prototypes. Accurate position hold capabilities allow an operator to e.g. capture high resolution imagery of the boiler surface and to traverse narrow passages. Fig. 2 indicates the position-hold accuracy achieved during experiments conducted shortly after the third integration week. Note that accuracy is influenced not only by the quality of the motion estimates, but also by external disturbances, communication and computation delays, vision-vehicle calibration, etc.

  A histogram of position errors will be generated to evaluate performance, from which key parameters such as RMS position error can be computed.

- *Trajectory following*: The second flight test will show the vehicle's capability to accurately follow reference trajectories in close proximity to the boiler surface. A pre-defined trajectory will be given prior to the flight test, and executed by the vehicle in an open-loop fashion (no obstacle avoidance). We aim to show the following: a) The vision/IMU module is able to cope with the dynamics of the vehicle (e.g. rapid rolling). b) Accurate trajectory following allows an operator to navigate in narrow, confined spaces such as in-between the superheater pipework. Those are the areas that are especially interesting for visual pre-inspection, as they are typically difficult to capture by 3D laser scanners from the ground.

  This experiment will also give an idea of motion estimation accurracy when the vision module is mounted on the vehicle. The quality of the inertial measurements degrades in the presence of vibrations, and motion blur may occur in the camera images. These effects cause less problems in hovering mode, as motion estimates are in this case always with respect to a single key-frame (thus no drift will occur). However, in trajectory following mode,

key-frames will be continuously introduced, and motion estimates will degrade more rapidly. Fig. 3 illustrates the scenario that the second flight test will resemble.

Deviation from the desired trajectory will be evaluated qualitatively for different trajectories and forward velocities.

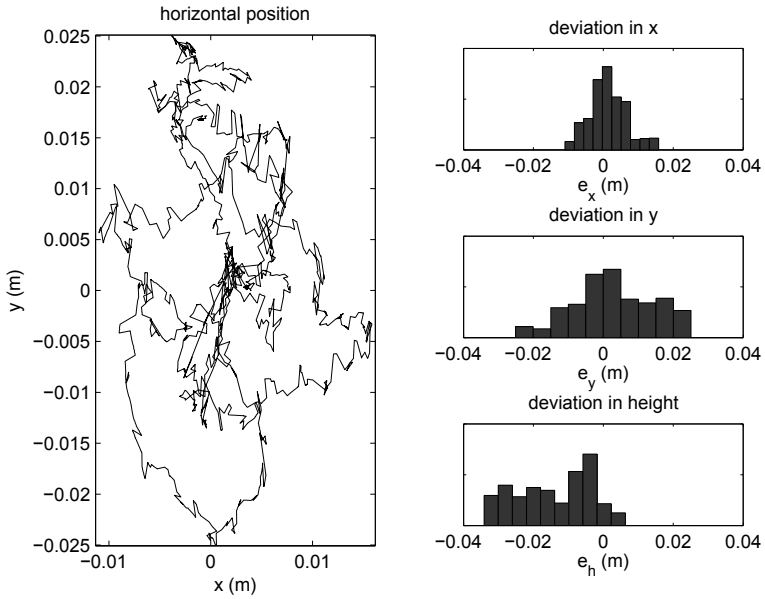

Figure 2: Deviation of the vehicle's position from a commanded, constant reference pose. Positive x indicates a deviation towards the mock-up.

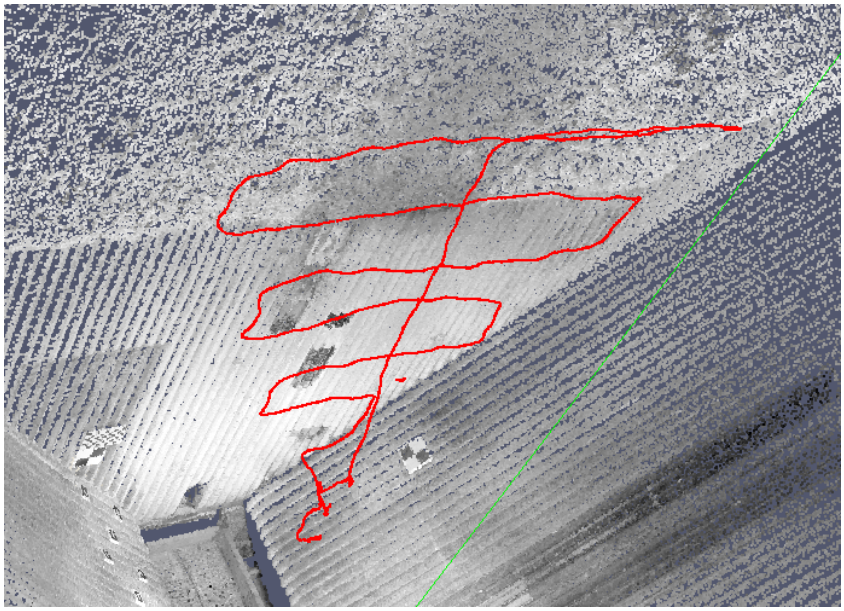

Figure 3: The second flight test will resemble actual AIRobots field tests conducted in the Narcea powerplant in June 2012. The vehicle will follow a pre-defined trajectory to simulate a "scanning" of the boiler's surface.

Autonomous Navigation and Planning

By exploiting the motion estimation capability described in the previous section, an additional inspection test will be performed in a fully autonomous way to demonstrate the autonomous capability of the system to reconstruct an unknown environment and hence to execute an high-level task. For this purpose, a wall recognition and reconstruction module will be employed in the real mockup scenario by using only egomotion measurements provided by the AIRobots stereo-Head. This module will provide in real-time the data need for the autonomous inspection task, that will be leaded by the high-level supervisory control. The preliminary test carried out with this new module has shown how the on-line wall reconstruction and estimation are performed with an accuracy suitable to accomplish an inspection task in a safe condition 4.

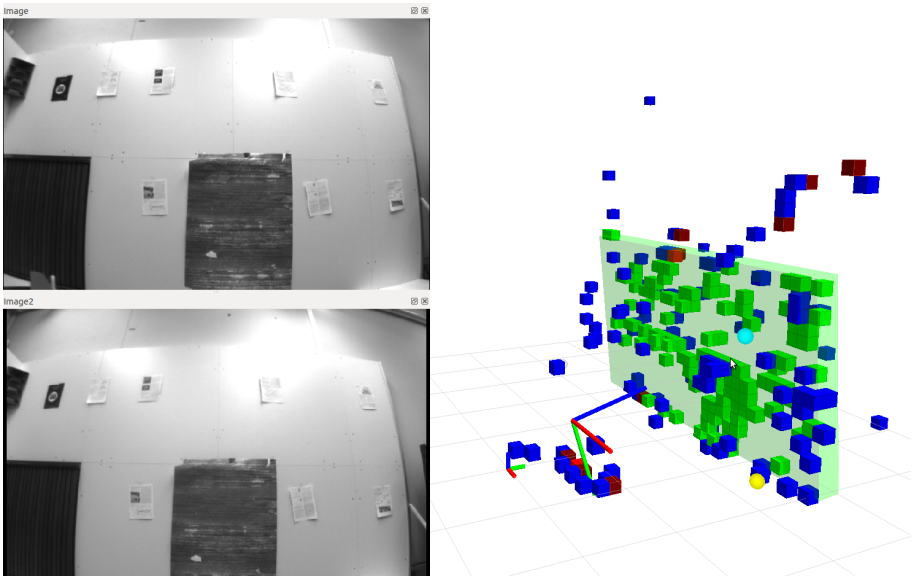

Figure 4: Wall reconstruction and recognition module working on real data.

Moreover, the presence of obstacles attached on the wall will could be explicitly considered as an advanced case. In this scenario, the desired system behavior should be the correct identification of the wall, by discarding the obstacles measurements from the data employed for the target wall reconstruction, and the correct identification of the obstacle in the occupancy map. In this way, the high-level supervisory control will be able to autonomous plan/replan online an inspection path for the observed wall.

3 Tele-Operated Inspection

Tele-Operated Free Flight

This experiment shows haptic teleoperation of a UAV during maneuvering and navigation (free-flight). It demonstrates how the haptic cues are effectively utilized to enhance the awareness of the operator about the current state of the UAV and the environment it is in. Specifically, a switching-based mapping and control methodology is realized to bridge the gap between workspace incompatibility that exists between the master and the slave devices and the required task-based precision. The robustness of the teleoperation control scheme to time varying delays, which are inevitable in real-time applications, are also illustrated.

Fig.5 - Fig.7 show results obtained during an intercontinental bilateral teleoperation of a quadrotor aerial vehicle in Computer Vision and Robotics Group of Australian National University commanded by an operator located in Robotics and Mechatronics Group of the University of Twente.

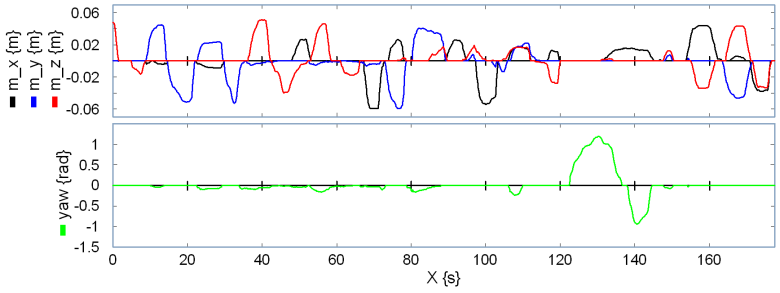

Figure 5: States of the master

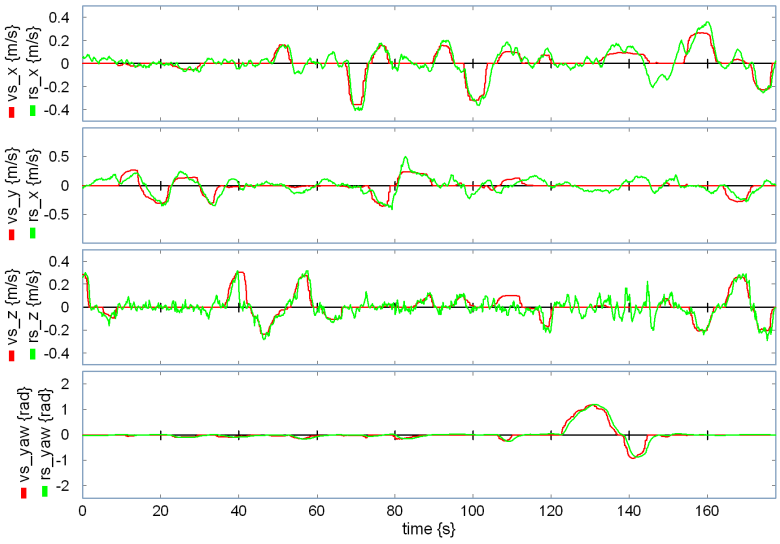

Figure 6: States of the real and virtual slaves

Tele-Operation in Contact with Environment

This part of the experiment shows haptic teleoperation of aerial vehicles with different configuration and low-level controllers both in free-flight and during interaction with the environment. The tests carried out in this subsection simulate a scenario in which the aerial vehicle is teleoperated by the operator for inspection by contact.

In the first test, a coaxial rotor craft from ETZ-Zurich with a hybrid pose/velocity/force low-level controller is integrated with the teleoperation framework developed by UT. During the experiment, the operator commands the Coax in free-flight from the starting position to the surface of the boiler to be inspected, while getting haptic cue on the states (position

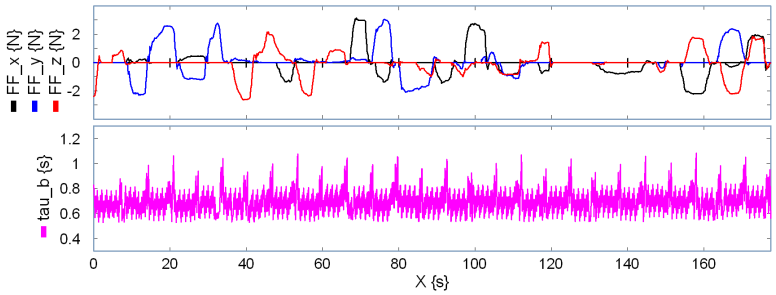

Figure 7: Force Feedback and time varying communication delay.

or velocity) of the UAV. Once the Coax docks to the surface of the boiler, the operator receives interaction force feedback in the direction normal to the docking surface. Fig. 8 and Fig. 9 show snap shots from the free-flight and interaction experiments during teleopera tion of Coax in the mock-up environment developed by AIR.

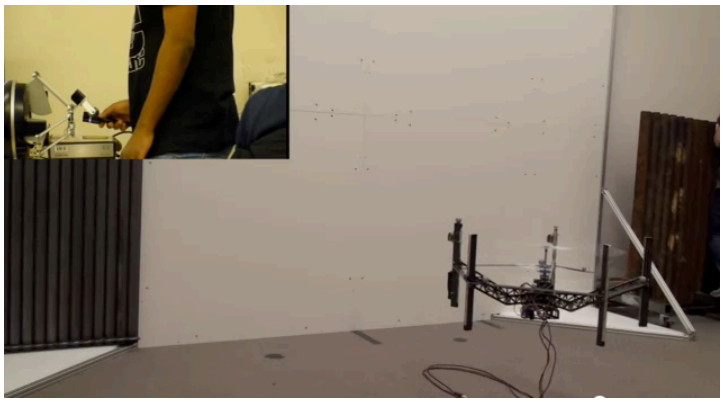

Figure 8: Haptic teleoperation of the Coax during free-flight

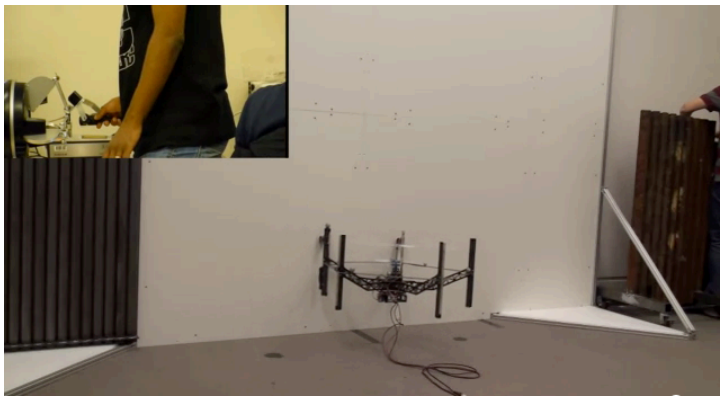

Figure 9: Haptic teleoperation of the Coax during sliding on a wall.

In the second test, a unified impedance-based teleoperation of a quadrotor aerial vehicle endowed with a robotic manipulator is performed. In this test, the operator commands the pose/velocity of the end-effector, both during free-flight and interaction. This test simulates high-level teleoperation of the end-effector, which is mostly the main point of interest, while hiding complex low-level dynamics of the UAV. It is important to note that the UAV is not necessary docked while the desired interaction task is carried out.

4 Surface Scanning by Contact

During the final review meeting, it is aimed to show the capabilities of stable physical interaction of the ACX (AIRobots Coaxial Helicopter) platform. According to the AIRobots spirit, the aerial vehicle has to be able to perform physical interaction in the sense of autonomous docking on vertical surfaces and to execute inspection maneuvers to detect crictical locations. The boiler mock-up specifically installed for AIRobots experiments is used as the experimental test-environment. In particular results related with autonomous maneuvering for transitioning between free-flight mode to docking mode and execution of wall-inspection maneuvers. Figure 10 presents a photo of the ACX while performing such a wall-inspection maneuver.

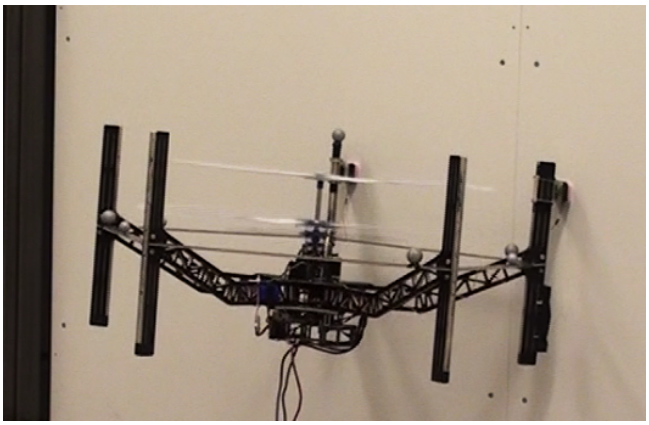

Figure 10: Photo of the ACX during force control on a wall

In further detail, the scheduled experiments will present the capabilities of the AIRobots CoaXial prototype as controlled by the hybrid predictive controller designed for free-flight navigation and physical interaction. According to the implemented approach, a unified constrained predictive control strategy computed over different modes of the system (free-flight, docking with upper points only, docking with both points and docking with lower points only) as shown in Figures 11. As intuitively understood, the ACX might collide initially with its upper point A (as seen in a 2-dimensional scenario) or with its lower point B, while the possibility of direct contact with both points is modeled as a sequential transition from the case of initial docking with point A and then with both in order to ensure the deterministic and well-posedness properties of the hybrid automaton.

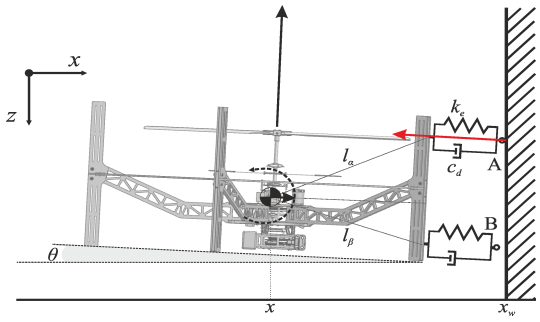

Figure 11: Illustration of the transition between free-flight and docking on a vertical wall

This modeling framework forms the basis for the computation of a hybrid predictive controller using an optimization framework to compute the control sequence of attitude references that can ensure optimal free-flight responses, safe transitioning to docking and sliding wall-inspection maneuvers while mainteining contact [**?**]. Response optimality is considered in the sense of the quadratic criterion. The derived controller is computed explicitly using mixed integer quadratic programming methods. The explicit controller is equivalent with its online counterpart in the sense that

they both provide the same control actions for the same input trajectories and therefore share the same stability and optimality properties. The computed attitude references are sent to the attitude controller which is based on coupled gain-scheduled proportional-derivative loops.

Example results of the main experimental scenario related with autonomous transition from free-flight to docking and performing sliding maneuver are shown in Figures **??** and 12. A video presenting such results can be found in the following URL: http://youtu.be/DRkILu7b-EQ.

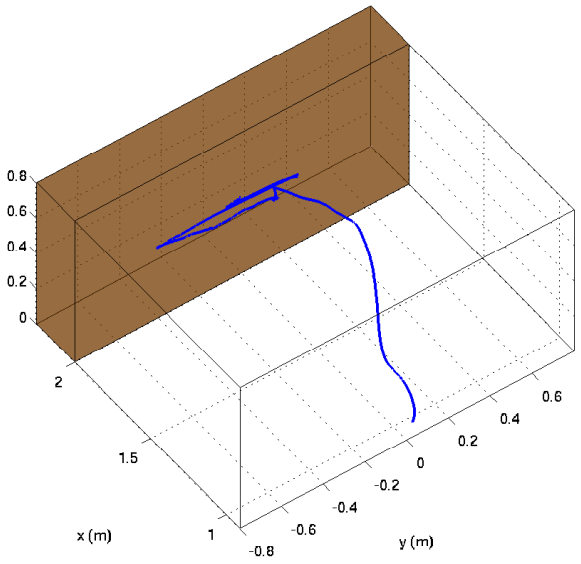

Figure 12: 3D view of a maneuver towards the wall, transition to docked dynamics and lateral sliding on the wall to perform an inspection mission.

As mentioned the designed control strategy is also capable of tracking free-flight trajectories. During such a test-case no switching between the hybrid modes takes place. Example results are shown in Figure **??**. Similar experimental test-cases will be presented during the review meeting for the final evaluation of the industrial inspection capabilities of the ACX platform.

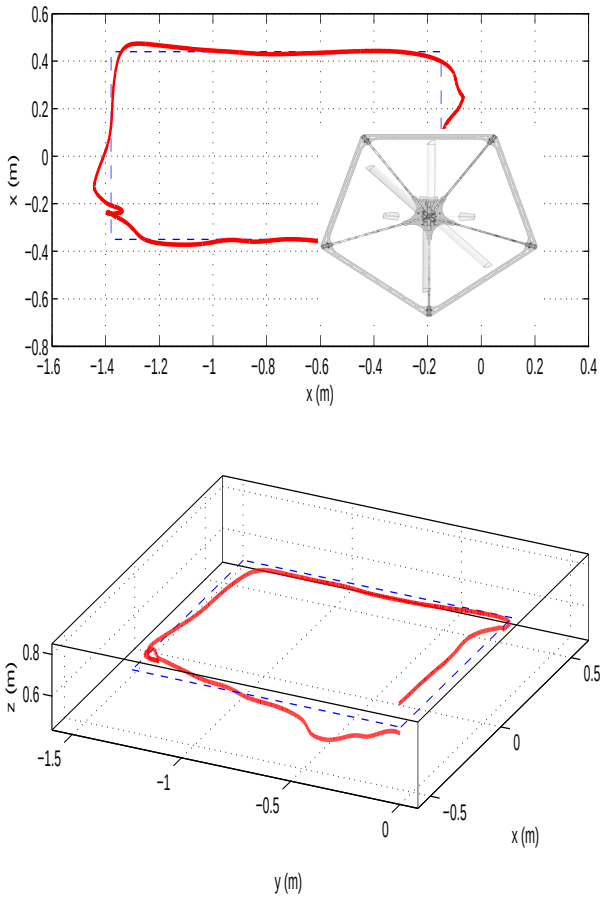

Figure 13: Trajectory tracking response. In the first part of the plot the ACX is presented in the same scale with the trajectory in order give a direct way to compare the dimensions and the fact that the trajectory is realtively narrow for a vehicle such as the ACX.

5 Aerial Manipulation

Autonomous Maneuvering in Confined Spaces

The goal of the this experiment is to test the performance of the autonomous navigation system at work in an unknown environment with the goal to reach a desired position to accomplish an inspection/manipulation task. In particular, our aim is to test the integration of autonomous (path/motion) planning, replanning, plan execution and mapping capabilities. The supervisory system generates a motion trajectory which is to be monitored and adapted during the execution when new obstacles are detected by the mapping process. To assess these capabilities we defined the following flight test: the vehicle should reach a final destination target avoiding an obstacle which is detected on the fly through the onboard cameras system (see Fig. 14). Specifically, in order to reach the final target, the high-level supervisory control has to replan a new trajectory on the fly (a new trajectory is computed from a switch point while old trajectory is still executed). On the other side, the low-level supervisor will plan the vehicle trajectory according to kinematic constraints. For example, if a replanning command is received when an obstacle is detected, a switch point between the old and new trajectory is computed while old trajectory is still executed. Then, the new trajectory starts in the switch point where the old and new trajectory have the same velocity ensuring the smoothness of the path transition.

Autonomous Aerial Manipulation and Inspection

Goal of this experiment is to evaluate prototype performances in achieving complex aerial manipulation tasks so as to demonstrate the effectiveness of the aerial platform in the inspection-by-contact scenario. The idea is to show how both the aerial platform and the onboard manipulator can be coordinated by the supervisor in order to accomplish the desired operation.

The high-level supervisor in particular is responsible to select the desired primitive (docking, free-flight, un-docking) and to generate the references for both the aerial vehicle and the manipulator.

The low-level controller, on the other side, has to maintain the stability of the overall system in the presence of contacts achieved with both the docking mechanism and the manipulator end-effector. Moreover the low-level controller has to guarantee the desired level of performance - in term of tracking precision of both the vehicle and the end-effector position - required to succeed in the specific operation.

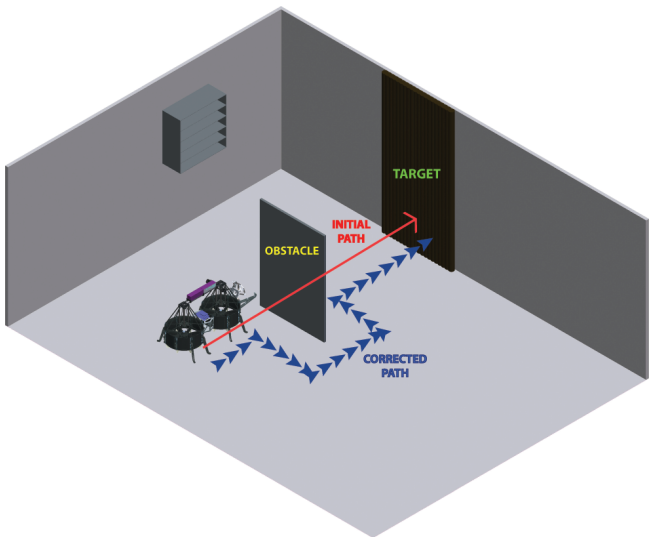

Figure 14: Autonomous maneuvering demo setup: in order to reach the desired target, the vehicle has to flight around the obstacle detected through the cameras. The supervisor is thus responsible of generating the corrected path.

The overall experiment will be then composed of the following steps:

- docking: in the first part of the experiment the supervisor select a position over the vertical surface that has to be inspected by contact. Accordingly, a suitable docking primitive is generated and performed by the low-level controller in order to reach the desired position, with a precision compatible with the limited workspace of the

onboard manipulator, and maintain a contact by means of the onboard docking mechanism. Docking operations can be repeated to employ the onboard manipulator on different parts of the mockup surface;

- manipulation: once the vehicle is attached to the surface in the desired position, the manipulator can be employed to achieve a certain task with a high level of precision. Two different manipulation tasks will be performed to evaluate the performances of the system in a real inspection-by contact scenario:
  - *aerial writing*: this part of the experiment is obtained by installing a proper tool on the end-effector in order to write a symbol on a desired portion of the mockup vertical surface. The idea is to show how the end-effector can be moved precisely along the surface similarly to an inspection-by-contact operation performed by means of NDT sensors. Once again, the high-level supervisor computes the desired path for the manipulator in order to accomplish the desired task, the low-level supervisor plans the manipulator trajectory while the low-level controller takes into account also for the stability of the vehicle in contact with the surfaces and of the forces applied to the environment in order to perform correctly the desired operation;
  - *probing*: in this task the manipulator is employed to probe a certain part of the of the mock-up selected by the supervisor. The idea is to show how the aerial manipulator can be employed to inspect portions of the mockup otherwise unreachable by the single aerial robotic platform.

Hybrid Interaction Control

This experiment demonstrates an autonomous hybrid interaction control strategy of an aerial manipulator. Impedance and force control modalities are implemented in the control scheme. In free flight, the manipulator is controlled in impedance mode. Whereas, during interaction, a force control along the axis normal to the surface of interaction is activated. During both flight regimes, the UAV base is controlled in impedance mode. The experiment simulates a scenario in which a task that requires force of different magnitude is carried out, while maintaining the possibility of moving along the wall. Fig. 15 shows a representative result.

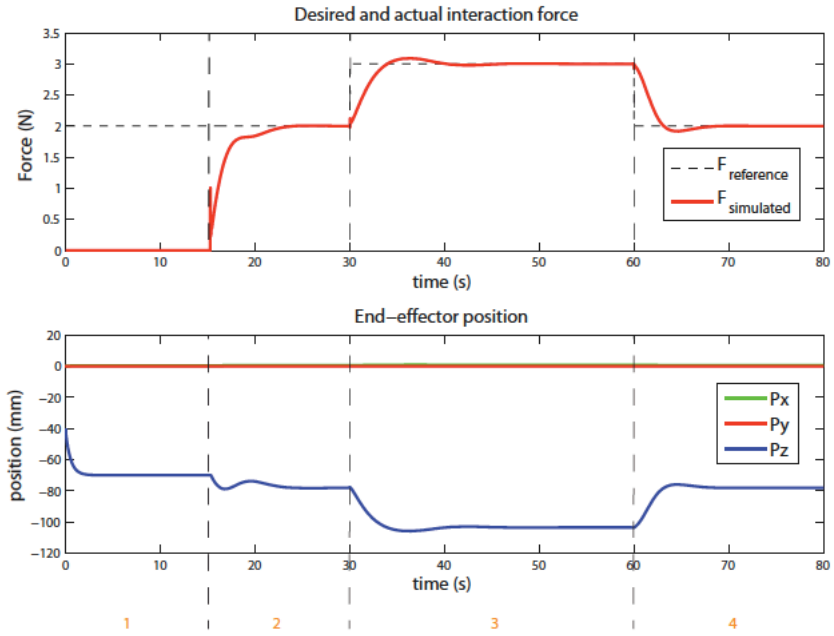

Figure 15: Results of the UAV endwed with the manipulator, showing the desired and actual interaction force and end-effector position.

Aerial Grasping

In this experiment, interaction control of a flying hand - composed of a UAV, a robotic manipulator and an underactuated gripper - is demonstrated. The experiment illustrates that the control strategy allows the flying hand to approach the wall, to dock on the object by means of the gripper, take the object and fly away. Fig. 16 shows two snap-shots of the flying hand while grasping a ball attached on a fixed all.

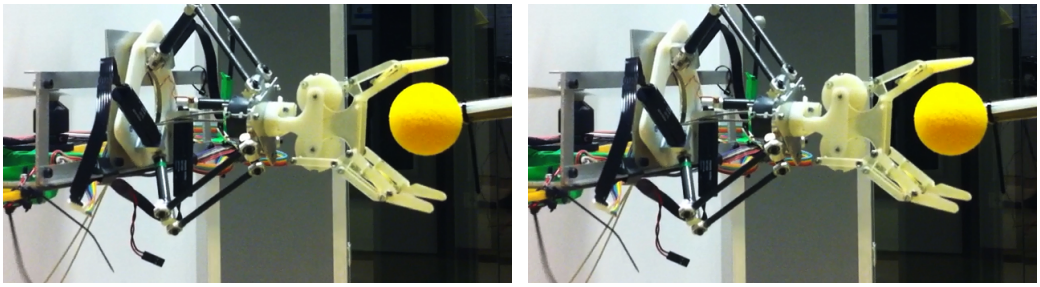

Figure 16: Two snap-shots of the flying hand in action.

6 Conclusion

Final conclusions are to be made after the actual demonstrations have been performed, evaluated and discussed with the review committee .